ROTATION PERIOD OF KORONIS FAMILY MEMBER (1442) CORVINA

Stephen M. Slivan
Massachusetts Institute of Technology,
Dept. of Earth, Atmospheric, and Planetary Sciences
77 Mass. Ave. Rm. 54-410, Cambridge, MA 02139
slivan@mit.edu

Francis P. Wilkin
Union College Dept. of Physics and Astronomy
Schenectady, NY

(Received: 2021 April 5)

We report lightcurve observations of (1442) Corvina made during 2021 March. Analysis of our data, together with constraints from survey "sparse" data recorded during the 2019 and the 2020-21 apparitions, yields an unambiguous rotation period of 77.92 ± 0.03 h.

We observed Koronis family member (1442) Corvina as part of an ongoing program to study rotation properties of the family's brighter objects (Slivan et al., 2008). In the literature we find no rotation period information for Corvina, making it the largest Koronis member lacking any period determination. Four nights of inconclusive unpublished relative photometry from near sea level in New England in 2012 did not show a clear brightness variation, suggesting a long period or a small amplitude.

To test for a long-period lightcurve of detectable amplitude we observed Corvina near its western stationary point in 2021 March, specifically to permit using the same on-chip field comparison stars over a series of nights, although it also limited the length of single-night spans of observability to about 5 h. Our observations were made on 9 nights over an 11-night interval (Table I) remotely using two telescopes operated by Telescope Live: SPA-2 in Oria, Spain, and CHI-1 in the Rio Hurtado Valley, Chile; details about both systems are summarized in Table II. A Sloan r' filter was used for all images, and image processing and measurement were as described by Slivan et al. (2008). To reduce systematic differences in the zero-points of our relative photometry from the two different detectors, we specifically chose comparison stars having similar color to Corvina's B-V = 0.87 ± 0.03 (Tedesco, 1989) based on the stars' photometry in the APASS DR10 catalog. Inter-comparison of the stars' brightnesses on our images confirmed no significant variation during our observing program.

UT date 2021	Tel. ID	Num. vis.	Obs. span (h)	SPA (°)	SPA corr. (mag)
Mar 11	SPA-2	1	0.36	15.3	0.000
Mar 12	SPA-2	1	0.36	15.5	-0.007
Mar 13	SPA-2	1	0.36	15.7	-0.014
Mar 14	SPA-2	1	0.36	15.9	-0.020
Mar 15	SPA-2	2	5.11	16.1	-0.025
Mar 17	SPA-2	1	0.36	16.5	-0.038
Mar 18	SPA-2	3	4.50	16.6	-0.043
Mar 19	CHI-1	1	0.16	16.8	-0.049
Mar 21	SPA-2	1	0.36	17.1	-0.058

Table I: Nightly circumstances. Columns are: UT date, telescope ID, number of observation visits made by the telescope, elapsed time spanned by the night's observations, solar phase angle, and brightness correction applied to correct for the change in solar phase angle since Mar 11.

Tel. ID	Dia. (m)	CCD camera	FOV (′)	Bin	Scale (″/pix)	Int. (s)
SPA-2	0.7	FLI-PL16803	29×29	2×2	0.86	120
CHI-1	0.6	FLI-PL9000	32×32	1×1	0.62	240

Table II: Telescopes and cameras information. Columns are: telescope ID, telescope diameter, CCD camera, detector field of view, image binning used, image scale, and image integration time used.

We reduced our Corvina observations for light-time and to unit distances, and for changing solar phase angle using the MPC adopted value of G = 0.15 for the slope parameter. The reduced photometry shows an overall brightness variation of about 0.2 mag which we conclude is due to the amplitude of Corvina's rotation lightcurve.

To identify candidate rotation periods, we used a "noise spectrum" approach, fitting a Fourier series model including through the 2nd harmonic to the observations to test a range of trial rotation periods. The search low bound is 18 h, which we estimate as the shortest period for a doubly-periodic lightcurve consistent with the 4.5-h span of (very slowly) increasing brightness that we detected on Mar 18. The search high bound is 300 h which is 2.5× the longest-period local minimum that we found at about 120 h. The resulting graph (Fig. 1, upper graph) shows four local minima candidate periods corresponding to roughly 0.4, 0.6, 1.4, and 1.6 half-rotations per day, all of which we individually confirmed are consistent with doubly-periodic lightcurves by inspection of the folded composites.

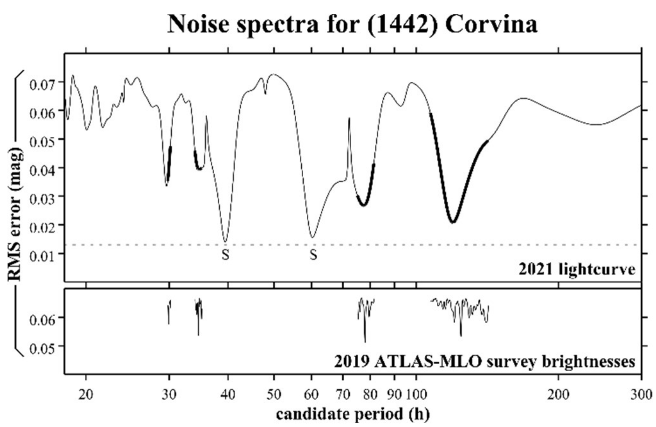

Figure 1. "Noise spectrum" graphs from fitting Fourier series models including through the 2nd harmonic, separately to two independent sets of photometry of (1442) Corvina. The upper graph shows the result from fitting to our 2021 lightcurve data, where the horizontal dashed line at 0.013 mag marks the mean of the nightly error bars on the photometry. The four ranges of periods that correspond to self-consistent doubly-periodic composites are highlighted in bold on the graph; the two remaining local minima marked "S" correspond to singly-periodic composites and were not further considered. The lower graph shows the result from fitting to ATLAS-MLO survey o-band brightnesses recorded during Corvina's 2019 apparition for the ranges identified by the upper graph, which refines the candidate periods.

Our data favor the two longer candidate periods over the two shorter ones, but in hopes of conclusively distinguishing which of the four is the true period we checked the asteroid brightness data that are publicly available online from the MPC astrometry Web site for additional observations. There we found suitable observations of Corvina from the ATLAS astrometric survey (Tonry et al., 2018), sparse in time but calibrated to a common brightness zero-point and available from both the 2019 and the 2020-21 apparitions. It is the

2019 ATLAS-MLO *o*-band data that have the most observations and cover the longest time span. We reduced those data for light-time and to unit distances, and for changing solar phase angle using a slope parameter value $G_o = 0.146$ which we obtained by fitting the Lumme-Bowell model to the reduced magnitudes. Fitting a 2nd-order Fourier series model to the reduced data for the period ranges determined from the 2021 lightcurves refines the candidate periods (Fig. 1, lower graph), but does not resolve the true period from the aliases because the photometry errors of about 0.04-0.05 mag limit the detectable level of self-inconsistency in the composite lightcurves.

Although ATLAS-MLO made fewer observations of Corvina during the following apparition in 2020-21 than it did during 2019, the later data still are sufficient for trial folded composite lightcurves. We reduced these data for light-time and to unit distances, reduced for changing solar phase angle using the slope parameter value determined from the 2019 data, and finally shifted the *c*-band data in brightness to composite with the *o*-band data.

We found that these 2020-21 data are less noisy than the 2019 data, enough that self-inconsistency of trial composites rules out the two shortest candidate periods, leaving only one alias still to distinguish from the true period.

There is additional information available from these data – because the longitude of the survey telescope at 156°W is very different from the 2°W longitude of the SPA-2 telescope that we mainly used for our own observations during the same apparition, the two data sets record different points on the rotation phase of Corvina's lightcurve. Thus, even though folding either data set individually at either remaining candidate period gives a self-consistent composite lightcurve, a mismatch in rotation phase of the composites folded at the same period would indicate an alias period. Comparison of the folded rotation phase for the two remaining candidate periods (Fig. 2) rules out 124.44 h, leaving only 77.96 h as being consistent with all of the observations from the 2020-21 apparition.

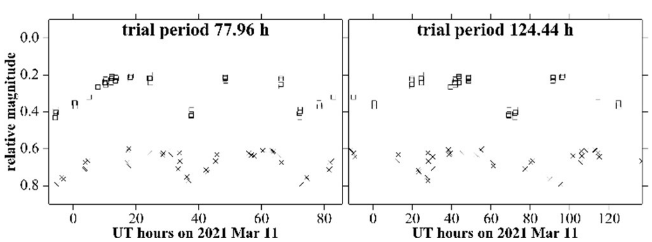

Figure 2. Lightcurves of (1442) Corvina during its 2020–21 apparition, composited to the same date and folded at two trial periods, for two independent sets of photometry: our lightcurve data (□), and ATLAS-MLO *o*-band and *c*-band survey brightnesses (×) combined for presentation. In the left graph folded at 77.96 h both composites share the same rotation phase, while in the right graph folded at 124.44 h the two composites are markedly out of phase, distinguishing that 77.96 h is consistent with the data but 124.44 h is not.

Having resolved the ambiguity in the period, we obtained our final result of 77.92 ± 0.03 h (Fig. 3) by fitting a 4th-order Fourier series model for the period to the combined data from the 2020-21 apparition, and estimated the error by adjusting the trial folding period to check self-consistency of the resulting composites.

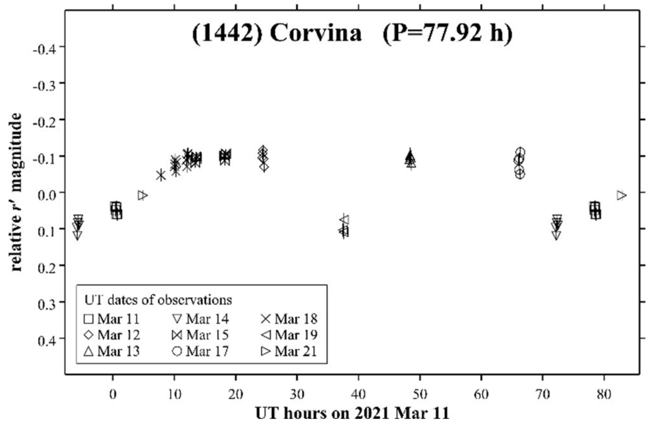

Figure 3. Folded composite lightcurve of (1442) Corvina during its 2020–21 apparition, light-time corrected, showing one rotation period plus the earliest and latest 10% repeated. The relative photometry was measured using the same comparison star on all nine nights; the asteroid brightnesses have been corrected for distance changes, and the solar phase corrections applied are given in Table I. Measurements from the 120-s images have been averaged so that each point on the graph represents an effective integration time of 240 s; the nightly error bars range from 0.008 to 0.018 mag.

Acknowledgments

We thank Marco Rocchetto for assistance with the remote observing. F. Wilkin received funding from the Faculty Research Grant at Union College. This work has made use of the AAVSO Photometric All-Sky Survey (APASS), funded by the Robert Martin Ayers Sciences Fund and NSF AST-1412587. This work also has made use of data and services provided by the International Astronomical Union's Minor Planet Center; specifically, the brightnesses accompanying astrometry from the Asteroid Terrestrial-impact Last Alert System (ATLAS) survey observing program.

References

Slivan, S.M.; Binzel, R.P.; Boroumand, S.C.; Pan, M.W.; Simpson, C.M.; Tanabe, J.T.; Villastrigo, R.M.; Yen, L.L.; Ditteon, R.P.; Pray, D.P.; Stephens, R.D. (2008). "Rotation Rates in the Koronis Family, Complete to $H \approx 11.2$." *Icarus* **195**, 226–276.

Tedesco, E.F. (1989). "Asteroid Magnitudes, UBV Colors, and IRAS Albedos and Diameters." In *Asteroids II* (R.P. Binzel, T. Gehrels, M.S. Matthews, eds.) pp 1090–1138. Univ. Arizona Press, Tucson.

Tonry, J.L.; Denneau, L.; Heinze, A.N.; Stalder, B.; Smith, K.W.; Smartt, S.J.; Stubbs, C.W.; Weiland, H.J.; Rest, A. (2018). "ATLAS: A High-cadence All-sky Survey System." *PASP* **130**, 064505.

Number	Name	yyyy mm/dd	Phase	L_{PAB}	B_{PAB}	Period(h)	P.E.	Amp	A.E.
1442	Corvina	2021 03/11-03/21	15.3,17.1	124	-1	77.92	0.03	0.19	0.02

Table III. Observing circumstances and results. Solar phase angle is given for the first and last dates. L_{PAB} and B_{PAB} are the phase angle bisector longitude and latitude at mid-date range.